Proceedings of ASME Turbo Expo 2011
GT2011
June 6-10, 2011, Vancouver, British Columbia, Canada

GT2011-46411

NUMERICAL SIMULATION AND FULL SCALE LANDING TEST OF A 12.5MW VERTICAL MOTORCOMPRESSOR LEVITATED BY ACTIVE MAGNETIC BEARINGS

Andrea Masala
Conceptual Advanced Mechanical Design
GE Oil & Gas, Florence, Italy

Giuseppe Vannini
Conceptual Advanced Mechanical Design
GE Oil & Gas, Florence, Italy

David Ransom
Southwest Research Institute,
San Antonio, TX, USA

Jeff Moore
Southwest Research Institute,
San Antonio, TX, USA

Luc Baudelocque
S2M
St Marcel, France

ABSTRACT

The development of a hermetically sealed, high speed, high performance motor-compressor for subsea application was started by GE Oil & Gas in 2006. The bearings consist of Active Magnetic Bearings (AMBs) as primary bearings and angular contact ball bearing pairs as auxiliary bearings, both provided by S2M. To mitigate the risk of rotor or stator component damage in case of a rotor emergency landing from full speed/full load conditions, a new numerical tool for predicting rotor and stator dynamics during the drop phase was developed in 2007 by GE Oil & Gas jointly with the Southwest Research Institute. In addition, a scaled vertical rotor drop test rig was built to validate the numerical tool, to perform endurance tests on the auxiliary bearings and to identify failure modes and relevant predictors.

The numerical tool was extended to predict the transient rotor drop dynamics of the full-scale prototype machine during field operation.

As a conclusion of the extensive factory acceptance test performed on the prototype machine, a rotor drop test with five drops on auxiliary bearings from full speed/full load was performed.

This paper presents the results of the experimental activity in terms of rotordynamic and auxiliary bearing performance. In addition, a comparison between measured and predicted parameters (i.e., rotor whirl frequency and amplitude) is discussed, highlighting the strong interaction between the axial and radial dynamics of the rotor on auxiliary bearings during coast-down. Finally, a detailed description of the post-test inspection of the auxiliary bearings and compressor internals is given.

GENERAL INTRODUCTION AND SUMMARY OF PREVIOUS EXPERIENCE

A hermetically sealed, high speed, high performance motor-compressor for subsea application has been developed by GE Oil & Gas. As gas field pressures drop and production rates begin to slow, subsea compression becomes a viable option for boosting the gas pressure at the wellhead on the ocean floor to maintain current gas production levels despite decreasing well pressure. Therefore, this unit is designed to operate on the ocean floor, providing natural gas compression for transport to an on-shore processing facility. Due to the significant cost of installing machinery in such a remote and challenging environment, system reliability becomes more important than for land based applications, and consequently, the requirement for the mean time between servicing (MTBS) has been set at five years or greater. For the mechanical design of the rotor-bearing system, this reliability will be achieved through a combination of active magnetic bearings with a “canning” system for additional protection against gas contaminants, and angular contact bearings for the auxiliary bearing system. Some of the other key design characteristics of the prototype include vertical rotor orientation, a direct coupled motor-compressor shaft, and three radial bearings, two on the motor shaft and one at the bottom of the compressor assembly. This arrangement has certain advantages, especially in terms of machinery footprint, protection from contaminants, and minimal maintenance requirements of mechanical elements.

For the auxiliary bearing system, the key to maximum life is to minimize the loads experienced by the bearings during an unplanned landing event, especially at full speed and full load. Starting in 2006, a development program was put in place to

achieve this design objective with the goal of being able to survive at least five full speed, full load landings without damage to the auxiliary bearing system or the rotor. For a vertical rotor orientation, auxiliary bearing loads are proportional to the radial clearance within the rotor-bearing assembly and the square of the rotor whirl frequency during a landing event. The whirl frequency is not the same as the rotating speed of the rotor, but rather is the frequency at which the rotor precedes around the bearing clearance while spinning at the shaft speed. As suggested by other authors [1] [2], forward whirl was expected for a vertical rotor during a drop onto the auxiliary bearings.

In the development program, a combined experimental/analytical approach was used to study the rotor landing event. A sub-scale test rig was built to develop a validated simulation tool in support of the full scale prototype development [3]. Unlike previous simulation approaches, the three-bearing flexible rotor and flexible stator scenario required the use of flexible body models for both the rotor and stator components in the simulation in order to fully capture the dynamics of the landing event. The experimental portion of the program provided the data necessary to validate the simulation, and the authors found behavior similar to that described by other researchers. In addition an endurance test campaign was carried out to determine the number of drops before encountering severe auxiliary bearing damage and to detect corresponding failure indicators [4].

The main finding of the experimental activity performed on the scaled test rig is that there is an unaccounted cross-coupled force leading the rotor into forward whirl. Through simulation, it was found that this cross-coupled force is likely very small, and could possibly be attributed to rotor damping and the non-synchronous response of the rotor to the transient landing event. In addition, it was determined by simulation that the whirl frequency increases with increasing cross-coupled stiffness. This is a new concept and is contrary to previous findings that associate whirl frequency with some structural mode of the stator. However, all of the previous work, including the more recent work performed on the three-bearing rotor system, is in the absence of any real fluid in the test rig housing (i.e., either vacuum or very low pressure). For the full scale Blue-C motorcompressor, the presence of cross-coupled forces due to impeller and seal rotor-stator interactions was predicted to significantly overwhelm any small amount generated by the damping in the rotor. From a design perspective, then the goal was set to minimize the cross-coupled stiffness not only for the traditional reason of rotor stability, but also for the purpose of minimizing the final whirl frequency of the rotor during a landing event.

Starting from January 2010, the Blue-C motorcompressor prototype went through an extensive test campaign to evaluate the system performance and reliability at different operating conditions [5]. In the present work, the results of the rotor landing tests, in which the rotor is dropped onto the auxiliary bearings from full speed and full load condition, is presented. These results include the rotordynamic response of the system and the performance of the auxiliary bearings. In addition, comparison is made between the numerical simulation predictions and the test results in terms of rotor whirl frequency and vibration amplitudes. Of special interest is the strong interaction between the axial and radial dynamics of the rotor during its coast down on auxiliary bearings.

NOMENCLATURE

AMBs: Active Magnetic Bearings
FAT: Factory Acceptance Test
M: modal rotor mass seen by each of the bearings ([kg])
e: rotor orbit radius during whirling ([m])
$\dot{\omega}$: whirling frequency ([rad/sec])
Pin: centrifugal compressor inlet pressure ([bar-g])
Pout: centrifugal compressor outlet pressure ([bar-g])
Tin: centrifugal compressor inlet temperature ([°C])
Tout: centrifugal compressor outlet temperature ([°C])
Qin: centrifugal compressor inlet volumetric flow ([m3/h])

LANDING TEST PROCEDURE

The landing test described below is part of a Factory Acceptance Test (FAT) program to qualify a motorcompressor prototype for the subsea compression application.
The motorcompressor vertical unit is rated at 12.5MW power and is composed of a high speed electric motor (located in the top section) which is rigidly coupled to a three-stage centrifugal compressor. The rotor is a single shaft running on three radial AMBs and one axial AMB (see Figure 1). The auxiliary bearings, which serve as a safety device in case of failure of the primary AMBs, are of the ball bearing type (a bearing pair, angular contact type). There is one auxiliary bearing with axial-radial capability located at the top of the rotor and the remaining two are just radial bearings. The damping source is a corrugated ribbon installed between the outer race and the fixed housing (see Figure 2). All the bearings (AMBs and auxiliary) were provided by S2M.

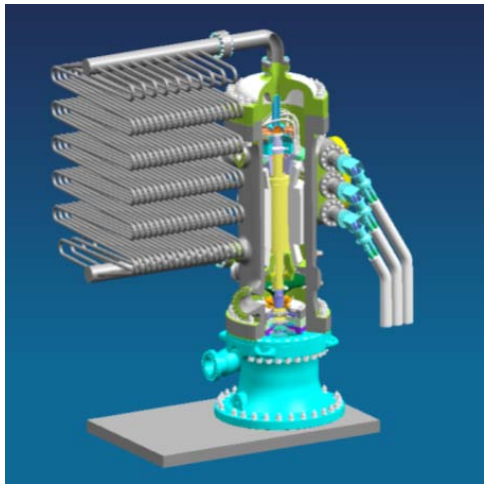

Figure 1 – Motorcompressor layout

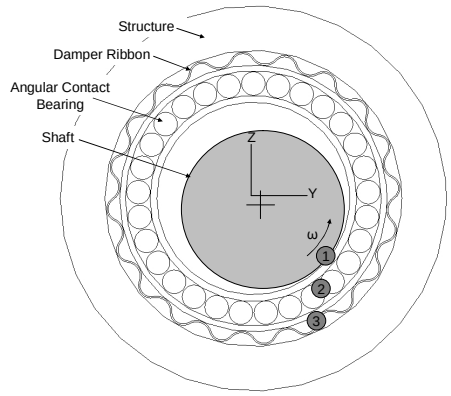

Figure 2 – Auxiliary bearing assembly schematic (S2M patent).

The FAT program was based on the following main steps:
- Mechanical Running Test
- Compressor Performance Test (ASME PTC-10 Type II)
- Full Load Test
- Full Speed Landing Test

The landing test was the last milestone in the test sequence in order to reduce the risk to the project. The landing test is very challenging due to the full speed, full power drop in a vertical configuration which has never been tested before, apart from the sub-scale testing done in SwRI [3]-[4].

The final purpose of the test was to prove that the system was able to sustain five full speed drops with no major damage. The number of drops in the test program was selected as a reasonable target to ensure the overall reliability of the plant.
In order to carefully analyze the consequences of each drop before proceeding to the next one, a comprehensive procedure was put in place which leveraged the available instrumentation and the lessons learned during the sub-scale testing performed in the SwRI laboratories ([3], [4]).
In terms of instrumentation it was possible to monitor the rotor displacements at each AMB location (very close to each auxiliary bearing section) through the feedback position sensors and the auxiliary bearing housing vibrations through dedicated accelerometers located at auxiliary bearings support flange.

To identify wear of auxiliary bearing components that may have occurred, a rotor clearance check feature was implemented in the S2M system in which the rotor was moved within the auxiliary bearing clearances to measure the clearance range variation. A rotor Transfer Function check on each bearing before and after each rotor drop was performed to identify any unusual modification of the rotor response or presence of debris between the rotor and stator.
Finally the overall rotor rundown time was also used as a rough indicator of possible bearing damage by comparison with the original time.

Due to the difficulty of quantifying reliable damage predictors for this transient landing event, the main objective was to compare each landing event to a baseline event, i.e., the first drop test, for all of the monitored parameters. In this way, the relative change in each parameter as compared to the baseline condition could be evaluated for signs of damage.
Finally the *GO-NO GO* criteria were defined as follows:
- Current auxiliary bearing clearances must be lower than 110% of the original clearances.
- Dynamic loads for each bearing ($M \cdot e \cdot \omega^2$) must be within safe limits (based on the auxiliary bearing dynamic capacity guaranteed by the manufacturer).
- Vibration amplitudes must be lower than half the AMB air gap.
- Accelerometer signals must not show major deviations from the original signature (from spectrum analysis).
- Rotor Transfer Functions detected by the AMBs must not show major deviations from the original status.
- Rundown time must be within ±10% of the original value.

On the basis of these criteria, each drop event was analyzed, and the detailed results and the main conclusions are described in the next paragraph.

ROTOR DROP TEST RESULTS

The rotor drop conditions were determined to address different requirements in terms of similarity to possible worst case drop scenarios in the field and the need to protect the machine during the landing phase. In particular, because no anti-surge protection system was implemented in the test facility, to prevent the machine from entering a risky surge regime during coast-down, a minimum separation margin of 15% from the surge line was maintained during machine coast-down.

Following the drop test procedure, a simulated drop test was performed to determine the machine's drop condition and to verify the proper separation from the surge line and rotor deceleration curve during coast-down. During this test, a trip command to the electric motor was given while the machine was operating at full speed and the desired drop test conditions, and the transient coast-down event was measured, while the rotor was still levitated by the magnetic bearings. The following observations were captured during the transient coast-down event, as highlighted in Figure 3:

1) Deceleration from 10160rpm to 3000rpm occurred in less than 10 seconds, confirming good agreement with predicted deceleration trend;

2) As result of the fast rotor deceleration, the discharge pressure of the compressor and the resulting pressure distribution across the compressor and electric motor changed rapidly during coast-down, getting to a uniform pressure across the machine close to the compressor suction pressure in less than 10 seconds upon trip event.

3) Due to the modified pressure pattern across the electric motor and compressor, two seconds after trip events the currents on the opposite halves of the axial AMB actuator, Z1 and Z2, became equal for approximately 5 seconds. During this

time frame the rotor weight load was balanced by the resultant gas pressure loads and the rotor continued spinning in a free hovering condition.

4) Motor-compressor thermodynamic measurements during the coast-down confirmed separation from the surge line.

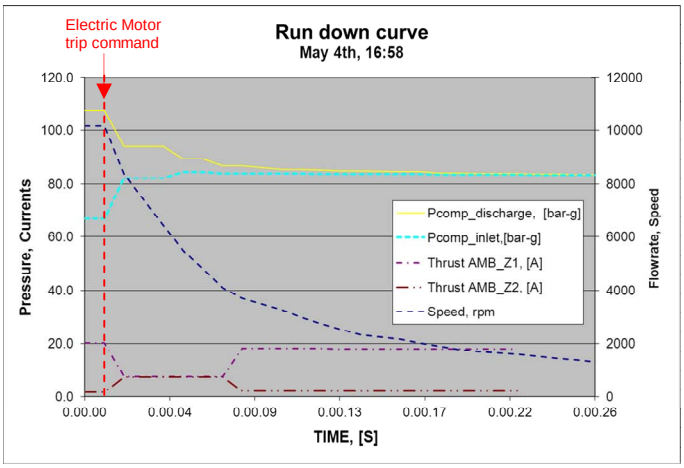

Figure 3 - Pressure, flow rate and axial AMB currents during coast-down.

Upon completing the preliminary checks, according drop test procedure, the five drops sequence from design speed and identified motor-compressor operating point was started: a 10 second overview of the vibration amplitude during deceleration is given in Figure 4. The following main events were captured:

a) Upon rotor delevitation (instant T1), the rotor deviated from the AMB constrained orbit and the displacement amplitude began to increase in both the radial and axial directions.

b) From instant T1 to instant T2 (~1sec) the electric motor kept running and providing positive torque to the rotor, whose speed remained constant at 10160rpm, as depicted in Figure 4(a);

c) During the T1 to T2 timeframe, the rotor dropped vertically downwards and developing a full whirl orbit in the radial direction;

d) As depicted in Figure 4(b), from instant ~T2 to T3 (~5 second time frame) the rotor moved upward with low acceleration/force (~0.1g /300N) confirming the rotor self-hovering effect already observed during the baseline rundown test;

e) At time instant T3 the axial force changed direction (due to reduced contribution of compressor pressure ratio as the rotor speed decreased) and the rotor again dropped vertically downwards under the effect of its weight load.

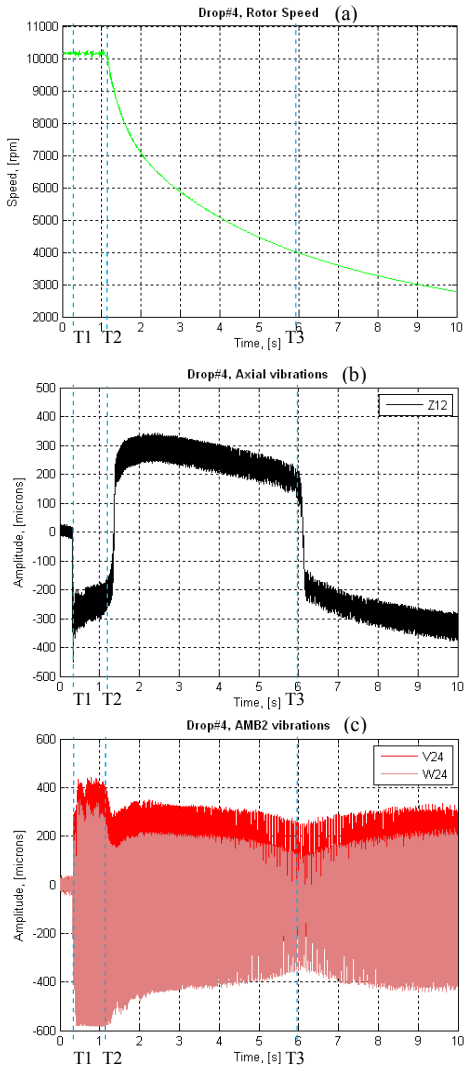

Figure 4: Rotor speed (a), axial displacement (b), and radial displacement (c) during 10 second drop.

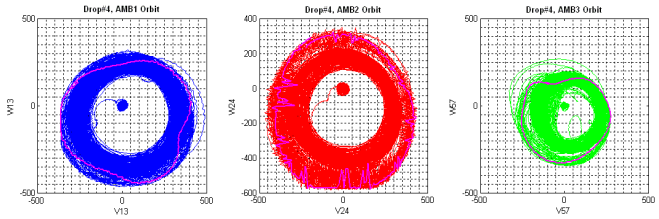

Figure 5: Radial orbits during coast-down

The rotor orbits in Figure 5 and the corresponding time signal highlighted that:

a) the rotor entered into a forward whirl motion as soon as the rotor was delevitated and it reached a fully developed whirl orbit in less than 0.1 second;

b) the whirl frequency stabilized to a frequency of ~40 Hz in less than 0.2 seconds after delevitation;

c) the rotor deflected shape was cylindrical (the vibration signal was always in phase for all position sensor axes).

The evolution of the whirl frequency during a drop event was captured by the Waterfall plot given in Figure 6.

- From time T1 to T2, when the rotor was running at maximum speed and the axial load was directed downwards and with magnitude comparable to the rotor weight, the whirl frequency and amplitude reached the highest values (450mm 0-pk@ 43 Hz on AMB1).
- From time T2 to T3, when the thrust load direction was inverted and the rotor spin speed started decreasing, the whirl frequency and amplitude decreased with rotor speed during coast-down.
- At time T3, when the axial load again changed direction and value (from +300 N to –18000N) the whirl frequency (and amplitude) increased from 25 Hz to 40Hz, while the rotor spin speed was decreasing.
- From time T4, approximately 15 seconds after T1, the rotor whirl frequency locked to the rotor speed while reaching the standstill operating condition.

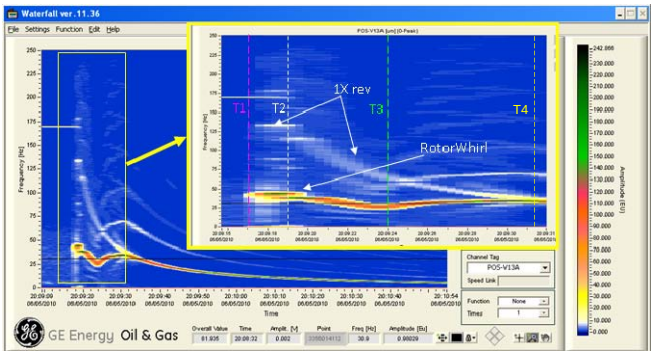

Figure 6 - Waterfall plot during drop test.

The rotor drop events and dynamics presented good repeatability for the five drops of the sequence, as summarized in Table 1, and no meaningful effect of auxiliary bearing degradation was noted.

Drop #	T1 [sec]	T2 [sec]	T3 [sec]	Max Whirl Freq [Hz]	Max Whirl Radial Amplitude, [µm] AMB1/AMB2/AMB3			Deceleration Time from 10160 (T_2) to 3000rpm
1	+0.12	+1.20	+5.8	43	490	550	350	8.056 sec
2	+0.33	+1.10	+5.7	43	480	539	300	8.257 sec
3	+0.27	+1.04	+5.4	42	400	449	280	8.267 sec
4	+0.32	+1.10	+6.0	42	410	400	250	7.958 sec
5	+0.17	+0.98	+5.8	42	420	450	260	7.977 sec

Table 1: Summary of drop tests

The fact that the rotor whirl frequency increases when the axial load was also increases, as highlighted at time T3, suggest that a strong coupling between the axial and radial dynamics of the rotor exist.

Similar phenomena had already been experienced during drop tests performed on the scaled test rig at the SwRI laboratories [3-4], when the rotor was delevitated only in the radial direction while the axial bearings maintained the rotor levitated.

The experiment highlighted that, compared to a full rotor drop (i.e., both in the radial and axial directions) the whirl frequency of the rotor changed from 90 Hz to 20Hz.

At that time, since no major aerodynamic effects were present in the system, the potential driver to forward whirl was identified to be the internal friction of the rotor, and the shift in the whirl frequency was attributed to modifications of the system internal friction due to changes in the contact pattern between the rotor and auxiliary bearings.

NUMERICAL SIMULATIONS

A comparison between the measured and predicted rotor drop dynamics is briefly described in this section to highlight how the numerical code for vertical drop prediction matched the experimental data and whether further actions to improve the numerical code for vertical rotor drop simulation are necessary.

To ensure equivalent experimental and simulation conditions, the following experimental inputs were implemented in the numerical code:

- Rotor deceleration curve matching the measured curve was included in the simulation (see Figure 7);
- Static axial load vs time, as per experimental measurements, was applied to the rotor during coast-down (see Figure 7);
- Seal coefficients calculated at the actual drop test operating conditions and different rotor speeds, with inputs derived from measured thermodynamic parameters;
- Unbalance level comparable to the unbalance present in the rotor, as estimated from rotordynamic assessment.

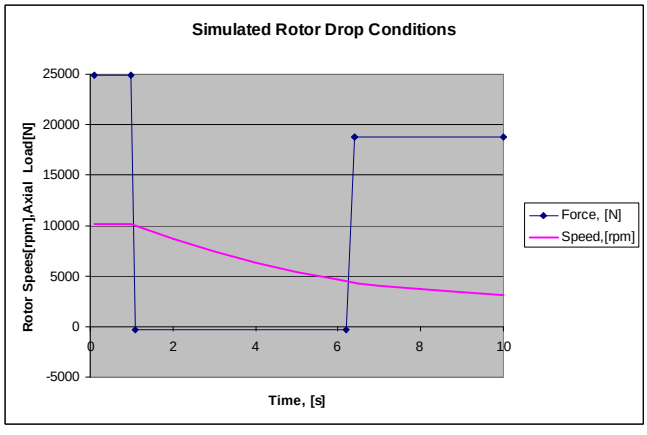

Figure 7 - Transient axial load and speed included in simulation.

A discussion of auxiliary bearings model and parameters effect on the simulation results was given in reference [4]. Based on the original numerical model and nominal parameters the following similarities with the experimental results were identified:

1) Predicted rotor whirl is forward and the amplitude increases in a first drop phase and then decreases with speed;
2) Highest vibration amplitude is on auxiliary bearing #2 and lowest is on auxiliary bearing#3;
3) Vibration amplitudes exceed the nominal clearance values (0.275 mm radial, including clearance and corrugated ribbon compliance) on the top and mid span auxiliary bearings.

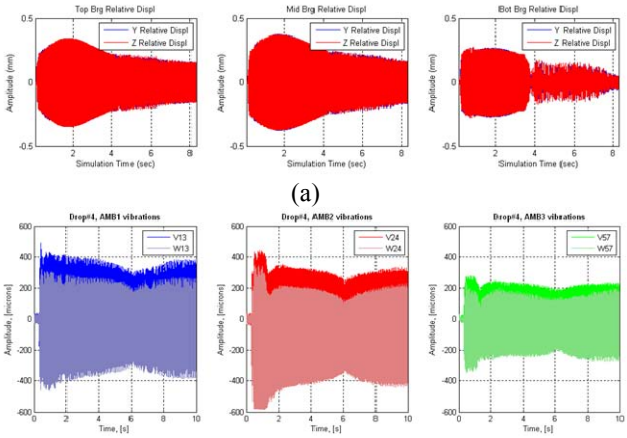

(a)

(b)

Figure 8: Comparison of simulated (a) and test (b) results

Important tips for further numerical model refinement and experiments were also provided by a detailed comparative analysis between numerical and experimental Waterfall plots (see Figure 8-b):

1) Compared to experimental results, maximum rotor whirl frequency was over-predicted (68 Hz vs 43 Hz): this can be related to conservative prediction of seals and canned AMB cross-coupling effects driving rotor into whirl;
2) Simulated whirl frequency increases in the first drop phase and decreases during rotor coast-down but at a lower rate than measured.
3) Whirl frequency is not significantly affected by axial load and dynamics: no whirl frequency increase was predicted at time T3 by numerical simulation, when the rotor dropped axially onto the auxiliary bearings after five seconds of self-hovering operation.

Further areas of research, as suggested to the authors by the experimental results mentioned above, will be covered in future works.

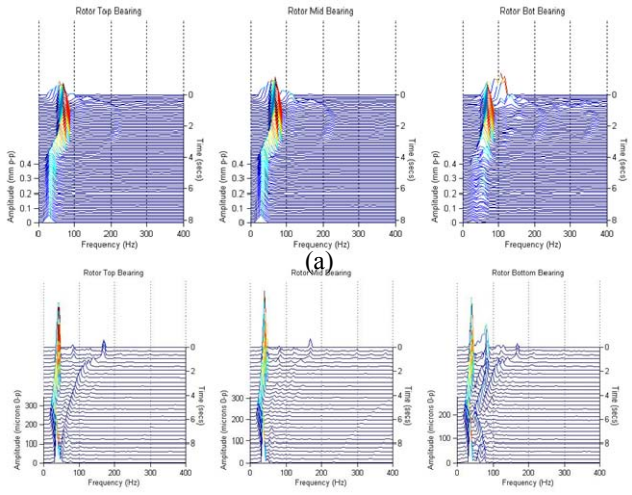

(a)

(b)

Figure 9 - Simulated (a) and tested (b) Waterfall diagram

POST TEST GENERAL INSPECTION

After the conclusion of the test campaign the motorcompressor was disassembled for a major inspection and especially to check the status of the auxiliary bearings and the stationary parts after the five full speed drops

Regarding the auxiliary bearings, the outcome of the inspection was positive since there were no signs of major damage on any of them. It was possible to free spin the bearing and the internal race surfaces (where the contact with the rotor occurred) looked quite smooth, having only minor rub marks. Finally the corrugated ribbon appeared to be in good condition, showing no heavy marks (see Figure 10).

No further investigation was done on these parts since they were replaced with new components and the general visual inspection was positive.

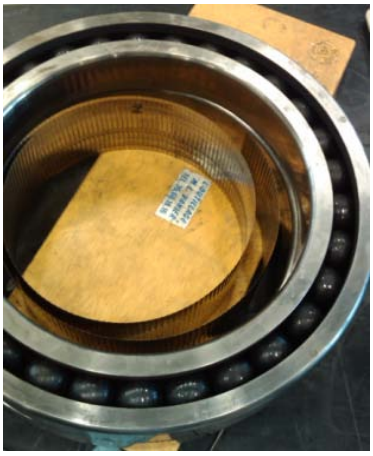

Figure 10 – Photo of auxiliary bearing with associated ribbon

As far as the motorcompressor stationary parts is concerned, the main interest was in checking the compressor internal seals since they are the stationary parts with the tightest clearances (except for the auxiliary bearings).

The centrifugal compressor bundle was completely dismantled to gain access to the internal seals.

The balance piston seal, which was of the honeycomb type, did not show any signs of rubbing. This was a very critical point during the design phase since the honeycomb performance (especially the rotordynamic coefficients) is affected significantly by a change in the clearance profile and the test proved the design to be robust (see Figure 11).

Regarding the other seals (labyrinth seals located either on the centrifugal impeller shroud or between two consecutive stages), a special design based on smooth stator parts made of abradable material and toothed rotor parts was adopted. This was decided both to leverage the centrifugal forces and reduce potential fouling during the operation, and also to increase the tolerance towards possible rubbing (possibly occurring during a landing event). The post-test inspection revealed no sign of rubbing (see Figure 11), proving that the selected seal clearance values were on the conservative side (they were about 1.5 times the auxiliary bearing clearances).

The rest of the motocompressor stationary parts (e.g., electric motor air gap and AMB stator parts) were also free from damage since all these parts had even higher radial clearances with respect to the rotor.

Overall, the landing test campaign proved the sound design of the auxiliary bearings-rotor system and their effectiveness in protecting the motorcompressor from high vibrations during the landing phase, at least for the five drops that were conducted.
The analysis of the test data showing a low level of variance and the post-test inspection showing no sign of severe damage are all good indications suggesting that the system could withstand an even greater number of drops at the same conditions. The maximum number of drops was not explored since it was out of the scope of the test program.

CONCLUSIONS

The landing tests performed on the subsea compressor prototype allowed full validation of the auxiliary bearings and rotor design and the positive results confirmed the endurance expected from dedicated sub-scale testing performed by the authors in the past [4].

From the analytical viewpoint, the tests showed that the predictive tool (which was set up by the authors to simulate the rotordynamic behavior during the landing transient) can be further refined to better reflect the whirling frequency.
However the tool proved to be capable of capturing some of the peculiar aspects of the landing phenomenon such as the direction of whirl, its amplitude and a conservative value of frequency.

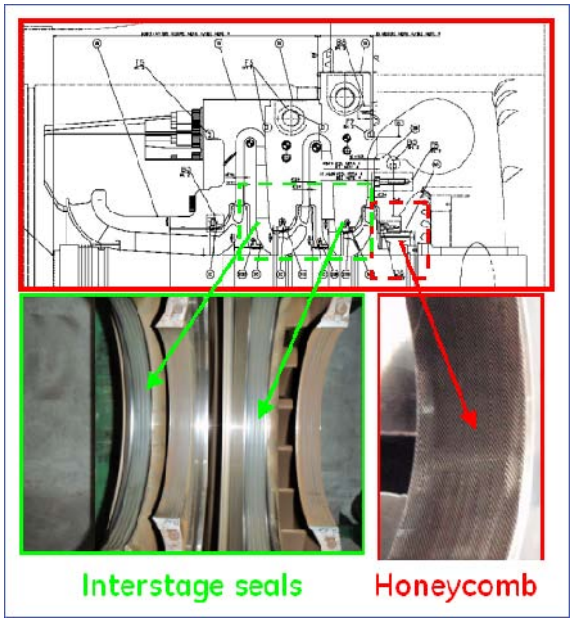

Figure 11 – Compressor internal seals.

ACKNOWLEDGMENTS

The authors thank GE Oil & Gas for allowing the publication of both the test results and comparison with predictions.
The authors would also like to thank the GE people from the Testing Dept. and the S2M people from the Field Assistance Dept., who made this testing possible.

REFERENCES

[1] - Spin commissioning and drop tests of a 130kW-hr composite flywheel, Caprio, M.T. – Murphy B.T. – Herbst J.D. – Proceedings of Ninth International Symposium on Magnetic Bearings (2004)
[2] - Flywheel Energy Storage System with AMB's and Hybrid Backup Bearings, McMullen P. – Vuong V. – Hawkins L., Proceedings of Tenth International Symposium on Magnetic Bearings (2006).
[3] - Numerical and Experimental Simulation of a Vertical High Speed Motorcompressor Rotor Drop onto Catcher Bearings - D. Ransom – A. Masala – G. Vannini – J. Moore - M. Camatti – Proceedings of 11th International Symposium on Magnetic Bearings (2008)
[4] - Development and Application of a Vertical High Speed Motor-Compressor Simulator for Rotor Drop onto Auxiliary Bearings – D. Ransom – A. Masala – G. Vannini – J. Moore - M. Camatti – M- Lacour – 38th Turbomachinery Symposium Proceedings 2009
[5] - Lateral rotordynamic analysis and testing of a vertical high speed 12.5MW motorcompressor levitated by Active Magnetic Bearings – A. Masala, – G. Vannini – M. Lacour – F.M. Tassel – M. Camatti – Proceedings of 12th International Symposium on Magnetic Bearings (2010)